Creep and Thermomechanical Fatigue of Functionally Graded Inconel 718 Produced by Additive Manufacturing

V. A. Popovich, E. V. Borisov, V. Heurtebise, T. Riemslag, A. A. Popovich and V. Sh. Sufiiarov

Abstract Inconel 718 is a nickel-based superalloy commonly used in aircraft engine and nuclear applications, where components experience severe mechanical stresses. Due to the typical high temperature applications, Thermo-Mechanical Fatigue (TMF) and creep tests are common benchmarks for such applications. Additive manufacturing offers a unique way of manufacturing Inconel 718 with high degree of design freedom. However, limited knowledge exists regarding the resulting high temperature properties. The objective of this work is to evaluate creep and TMF behaviour of Inconel 718, produced by selective laser melting (SLM). A novel microstructural design, allowing for grain size control was employed in this study. The obtained functionally graded Inconel 718, exhibiting core with coarse and outside shell with fine grained microstructure, allowed for the best trade-off between creep and fatigue performance. The post heat-treatment regimens and resulting microstructures are also evaluated and its influence on creep and TMF is discussed.

Keywords Additive manufacturing · Inconel 718 · Functional grading Creep · Thermo-mechanical fatigue

V. A. Popovich (✉) · T. Riemslag
Department of Materials Science and Engineering,
Delft University of Technology, Delft, The Netherlands
e-mail: v.popovich@tudelft.nl

E. V. Borisov · A. A. Popovich · V. Sh.Sufiiarov
Peter the Great Saint-Petersburg Polytechnic University, Saint Petersburg, Russia

V. Heurtebise
SIGMA Clermont, Cedex, France

Introduction

Inconel 718 is a precipitate strengthened nickel-based superalloy, which is commonly used in aerospace applications, where severe mechanical and thermal stresses are induced on a component. Inconel 718 is characterized by high strength, excellent creep, oxidation and corrosion resistance up to 700 °C, making it suitable for turbine, jet engine and nuclear reactor applications [1–3].

Conventional manufacturing routes of nickel-based alloys include casting, forging and powder metallurgy. However, near net shaping of complex components is difficult using such methods [4]. Recently, additive manufacturing (AM), such as selective laser melting (SLM), received a lot of attention, as it allows for several advantages compared to conventional technologies, like reduction of production steps, high flexibility, low material consumption and, most importantly, the possibility to manufacture parts with high geometrical complexity and dimensional accuracy [5, 6].

It is known, that the grain size is a typical way of controlling mechanical properties, including those of Inconel alloy 718 [7, 8], where coarser grained microstructure is favoured for creep strength and crack-growth resistance, while finer-grained structure for better fatigue life and tensile yield strength. In our previous study [9], a novel functionally graded Inconel 718 was produced with local functionalities via crystallographic texture, grain size and anisotropy optimization. It was shown that the grain structure and crystallographic texture of Inconel 718 can be changed during SLM processing by adapting the scanning strategy and the local solidification conditions. Furthermore, the effect of heat treatment has been investigated [10] and the results showed the capability of the SLM process to produce parts with mechanical properties better than conventional Inconel material.

The aim of this study is to investigate high temperature mechanical behaviour, such as creep and thermo-mechanical fatigue in order to fully explore the benefits of microstructural design in SLM Inconel 718. The effect of heat treatment on microstructure and high temperature mechanical behaviour is also evaluated and compared with conventional wrought Inconel 718.

Experimental Details

Materials and Heat Treatment

For manufacturing of the SLM specimens, (see Table 1 for process parameters) an SLM 280^{HL} facility (SML Solutions Group AG, Germany) featuring two YLR-lasers with a wavelength of 1070 nm and a maximum output power of 400 and 1000 W was employed. Laser power of 250 and 950 W was used to produce different areas within functionally graded cylindrical rods of 140 mm × Ø 14 mm (Fig. 1), further referred as FGM samples. The Z-axis was defined parallel to the

Table 1 Process parameters applied for SLM fabrication of specimens [10]

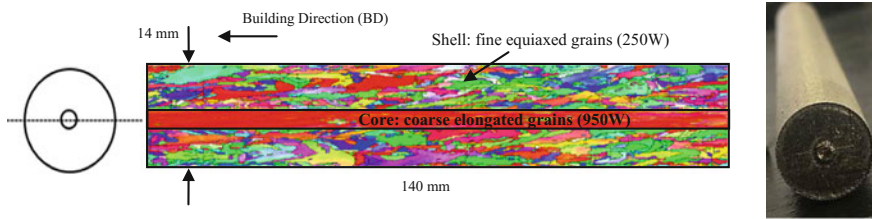| Laser power (W)	Laser scanning speed (mm/s)	Hatch distance (mm)	Layer thickness (μm)	Volume energy density (J/mm^3)
250	700	0.12	50	59.5
950	320	0.5	100	59.4

Fig. 1 SLM fabricated functionally graded Inconel 718 using a variation of 250 and 950 W laser sources

building direction, whereas each layer was deposited parallel to the XY-plane with the laser scanning at 45° between X and Y.

Post heat treatment was applied to examine the effect on microstructure and mechanical properties of Inconel 718 with tailored microstructure. The samples were investigated under "as-processed" and "heat treated (HT)" conditions, complying with AMS 5664E requirements [11] (see Table 2 for heat treatment details). In order to avoid contamination with oxygen, all heat treatments were conducted in argon atmospheres.

Samples of each of the heat treated conditions taken from YZ and XY planes were prepared for microstructural examination by grinding and polishing down to 1 μm. In order to reveal grain size and morphology, the specimens were etched in Glyceregia reagent (15 ml HCl, 10 ml glycerol and 5 ml HNO$_3$). Optical microscopy was carried out on a Keyence VHX-5000 for microstructure and porosity

Table 2 Designation of specimens and heat treatment parameters used for Inconel 718

Designation	Heat treatment	Details
As-processed (AP)	–	250, 950 W or Functionally Graded (FGM), see Fig. 1
Heat treated (HT)	Annealing + Aging	• Annealed at 850 °C, 2 h (air cooling) • Aged for 8 h at 720 °C, furnace cooling to 621 °C and holding for 8 h followed by air cooling
Wrought Inconel 718 (Wrought)	Annealing + Aging	• Solution annealed at 955 °C (1 h) • Aged for 8 h at 720 °C and furnace cooling to 621 °C and holding for 8 h followed by air cooling

investigation. A JEOL JSM 6500F scanning electron microscope (SEM) with energy-dispersive spectroscopy was used for fracture surface analysis. Vickers hardness profile measurements were performed under 3 kg force (further denoted as HV_3). X-ray diffraction (XRD) patterns were obtained using Brukker D8 diffractometer with CoK_α radiation ($\lambda = 1.79020$ Å). Diffraction patterns were recorded within the 2θ range from $10°$ to $120°$ with a step size of $0.035°$. The X-ray beam was collimated to a spot size of 3 mm in diameter on the sample surface.

Creep and Thermomechanical Fatigue Testing

For creep and Thermo-Mechanical Fatigue (TMF) testing the round dogbone specimens were machined parallel to building direction as shown in Fig. 2a. Creep rupture and TMF testing were conducted on a servo hydraulic MTS 858 Table Top System, where induction heating and forced air cooling are used in order to cycle the temperature, Fig. 2b. During the tests the temperature was controlled by three thermocouples, which were in contact with the gauge of the specimen. The strain was monitored by the ceramic rod extensometer.

Creep rupture tests were performed at a constant tensile stress of 690 MPa and temperature of 650 °C, according to ASTM E139 standard [12]. Average creep properties were calculated based on 3 samples tested per process condition. After creep rupture the samples were prepared for fractography analysis.

Strain controlled in-phase thermo-mechanical fatigue (IP-TMF) tests were performed with temperature cycling between 350 and 650 °C at a frequency R = $\varepsilon_{min}/\varepsilon_{max}$ = −1 and a strain amplitude of ±0.45%. Strain was measured by an axial extensometer and all tests were done in mechanical strain control (i.e. with a fixed total strain range compensated for thermal expansion $\Delta\varepsilon = \varepsilon_{max} - \varepsilon_{min}$). TMF testing was performed per process condition at a cooling and heating rate of 1 °C/s with a holding time at T_{max} of 300 s.
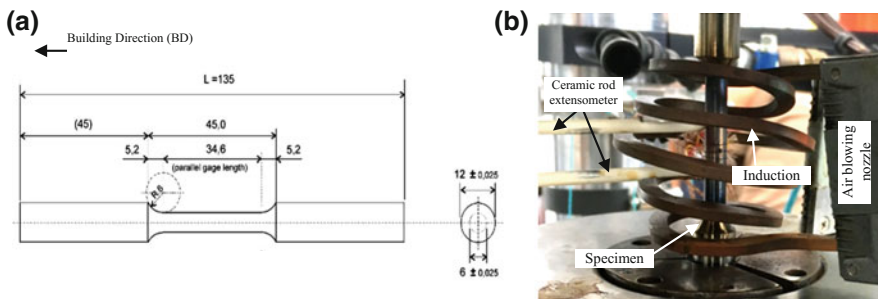

Fig. 2 Schematic of the creep and TMF test specimen and high frequency setup

Results and Discussion

Microstructural Characterization

Figure 3 shows optical microscopy images of the microstructure of Inconel 718 samples processed with the 950 and 250 W laser sources, further referred to as 950 and 250 W samples. As can be seen, the 250 W samples show a finer grained microstructure compared to the samples processed with the higher energy laser (Fig. 3a and b). Furthermore the microstructure of the part built with the 950 W laser (Fig. 3b) shows the formation of large columnar grains, primarily aligned along the building Z-axis with long axes approach the millimetre length range. In our previous study it was shown that columnar grained region has elongated grains with a (001) orientation with respect to building direction, i.e. the direction of predominant heat flux during processing. The observed microstructural differences were used to develop functional materials by modulating the laser scan strategy and process parameters [9] and resulting in a material featuring the core produced with coarse grains, while shell with fine grained microstructure (Fig. 3e, top view).

As previously shown, there is a formation of NbC and Laves-phase particles in the as-processed material [10]. Laves usually forms in heavily segregated regions and is known to reduce the mechanical properties of Inconel 718 through several mechanisms with the most dominant being brittle fracture of the phase, that provides the conditions for nucleation and crack growth. The presence of Laves phase in as-processed condition was further confirmed in this study by XRD, see Fig. 4.

In order to avoid the occurrence of such undesired microstructural features, post-processing heat treatment in a form of solution treatment and double aging were performed. The microstructure after heat treatment (see Fig. 3c, d, f) maintained its columnar nature and traces of layered build up. Furthermore, as can be seen in Fig. 3d, 950 W condition shows considerably larger process induced defects. The Laves phases on the other hand seem to transform into a needle-like Ni_3Nb-δ precipitates [10], which in this study is supported by XRD spectrum shown in Fig. 4.

Porosity measured by optical metallographic method showed that there is four times more porosity in 950 W samples ($\sim$4.5%) as compared to 250 W ones ($\sim$1.1%), which is considered as process induced defects and its detrimental effect on mechanical performance will be discussed in the next section.

Creep and Thermomechanical Fatigue Testing

Creep, porosity and hardness results for all tested materials are shown in Table 3, where t_f is the final time of fracture, ε_f is fracture strain and ε'_s is steady state creep rate. As expected [13, 14], the coarse grained microstructure is more creep resistant with respect to fracture strain (by a factor of three for heat treated condition).
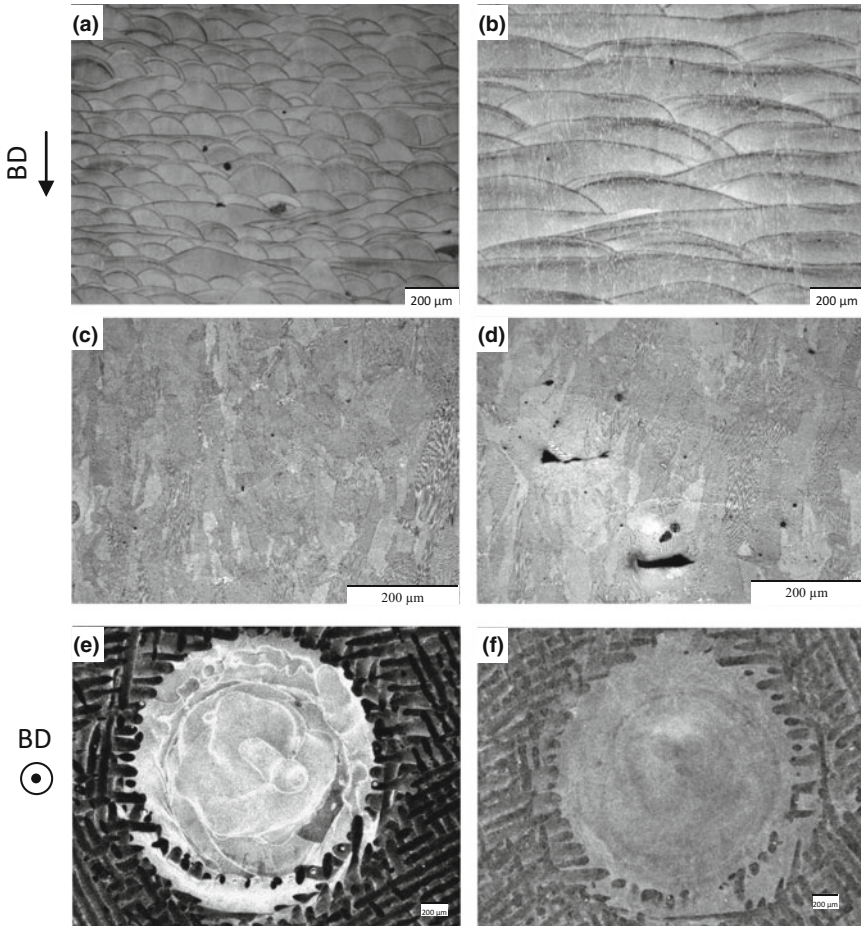
Fig. 3 Optical micrographs of SLM Inconel 718 specimens: **a** and **b** as-processed 250 and 950 W; **c** and **d** heat treated 250 and 950 W; **e** and **f** as-processed and heat treated functionally graded material. Images (**a**)–(**d**) depict top YZ plane, while images (**e**)–(**f**) show top XY plane, with 950 W zone located in the core

However, due to high scatter in results no clear conclusions can be drawn regarding the other creep parameters, such as creep life. It is believed that the high scatter is caused by the larger amount of process induced defects (porosity) observed in 950 W samples. The other explanation could be that in this temperature and stress range there is no grain size effect and a further research at lower stress and temperature level is recommended in order to evaluate the possible threshold level.

As can be seen, heat treatment substantially improves creep properties of SLM produced material. An increase of hardness by 40% for the as-heat treated condition is most likely attributable to precipitation hardening by plates of δ-phase (see Fig. 4 and [10]), which acts as a barrier for dislocation motion, thus improving hardness
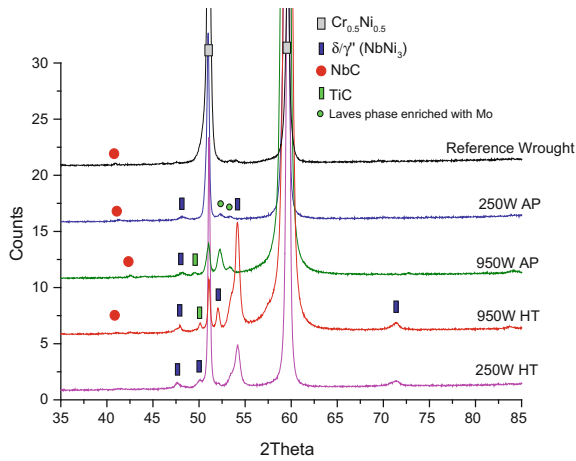
Fig. 4 XRD patterns showing reference wrought Inconel 718, as-processed (AP) and heat treated (HT) Inconel 718 produced via SLM with 250 and 950 W laser sources

Table 3 Creep results for 650 °C at a stress of 690 MPa

Specimen	t_f (h)	ε_f (%)	ε'_s (1/h)	Porosity (%)	Hardness, HV_3 250 W/950 W
250 W–AP	0.04 ± 0.04	15.6 ± 0.067	3.984 ± 2.70	1.1	303
250 W–HT	1.43 ± 0.58	4.0 ± 0.006	0.014 ± 0.006	1	446
950 W–AP	Fractured before reaching maximum stress of 690 MPa			4.5	290
950 W–HT	1.23 ± 0.80	12.3 ± 0.057	0.031 ± 0.034	4.1	415
FGM–AP	0.17 ± 0.18	17.3 ± 0.062	1.596 ± 1.491	0.3	312/294
FGM–HT	0.53 ± 0.23	9.0 ± 0.014	0.071 ± 0.031	0.4	449/426
Wrought	25.27 ± 10.32	18.8 ± 0.066	0.004 ± 0.001	0.2	424

and creep properties. Conversely, a significant reduction in creep fracture strain, can be explained by the presence of large carbides. As discussed in work [15], at this high temperature level, creep properties of Inconel alloy rather depend on applied stress than the grain size. Hence, for these testing conditions, heat treatment seems to be the most dominant factor controlling the creep life of SLM produced material. Furthermore, when compared with the reference wrought Inconel, it is evident that the lifetime of AM material should be significantly improved, which might be possible by reducing process induced defects. Hence, for final application of the higher energy laser source it is required to further optimize processing parameters and/or apply post processing hot isostatic pressing in order to reduce porosity.

Fracture surface of crept specimens is shown in Fig. 5. As can be seen, wrought Inconel exhibits ductile fracture with characteristic dimpled fracture and typical microvoid coalescence (Fig. 5a and b). SLM Inconel produced with 250 W

(fine grained microstructure) shows signs of ductile fracture with areas of cleavage planes associated with the location of brittle Laves phases (Fig. 5c and d). Inconel produced with 950 W (coarse grained microstructure) failed before reaching maximum stress level. Fracture surface of this material exhibits process induced pores and defects, which serve as stress concentrations inducing premature failure and thus resulting in interrupted creep test and thus p its poor creep properties (Fig. 5e and f).
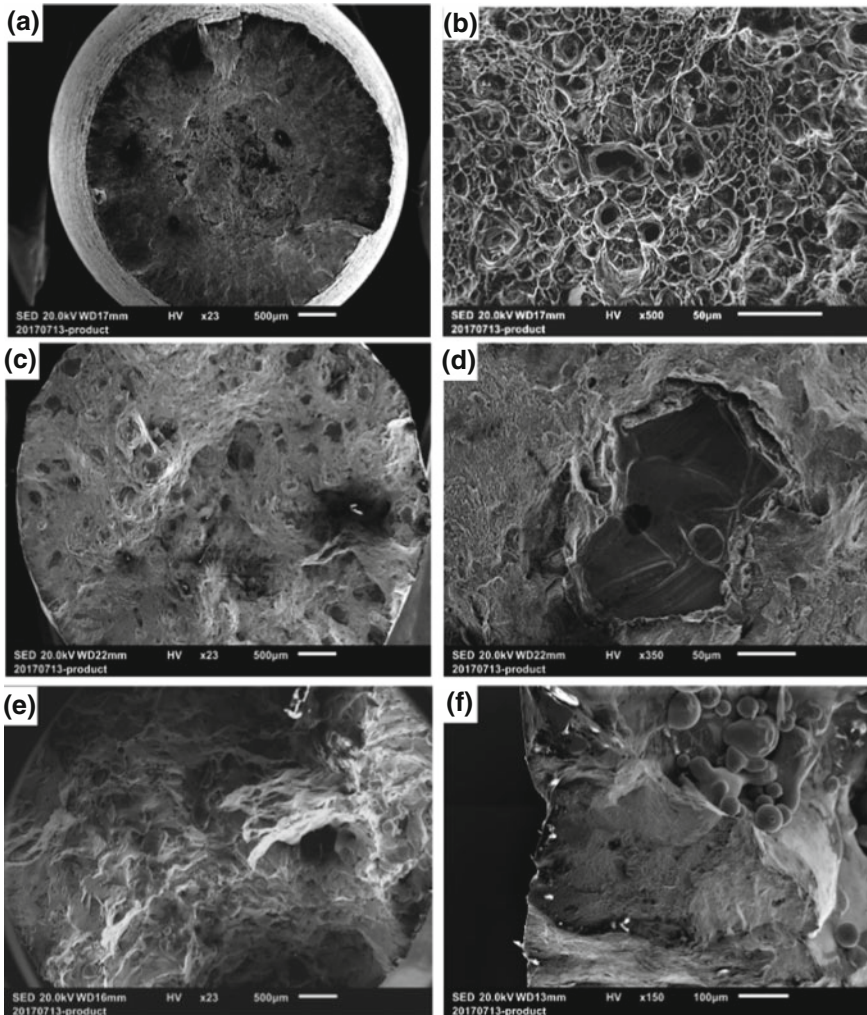

Fig. 5 Fracture surface of Inconel 718 after creep test at 650 °C and 690 MPa: **a** and **b** Wrought Inconel; **c** and **d** SLM produced with 250 W; **e** and **f** SLM produced with 950 W

Fractographic images of heat treated and FGM samples are shown in Fig. 6. One can see that 250 W (fine graded microstructure) has intergranular fracture with secondary cracks initiating at the grain boundaries (Fig. 6a and b). Parallel slips appearing within the same grain and cracks visible near the boundary (Fig. 5b) confirm a typical appearance of pure creep fracture surfaces. Contrary to 250 W specimens, 950 W condition shows microvoid coalescence indicating ductile mode, which might be attributed to the high density of process induced defect, resulting in insufficient time for creep mechanisms initiation. It should also be noted, that 950 W specimens have a coarse grained microstructure with grain orientation parallel to loading direction and there might be no grain boundaries present in the highest stress area (corresponding to pores and inclusions, see Fig. 7b). This observation is further confirmed in FGM samples (Fig. 6e–g), showing a clear transition, indicated by the black dashed line, from intergranular fracture (outside shell corresponding to 250 W) to ductile fracture (core corresponding to 950 W). A cross sectional investigation of crept specimens cut along the loading direction is advised for future work in order to get a deeper understanding of creep damage mechanisms acting in SLM processed material.

Thermomechanical fatigue (TMF) testing was performed in order to get closer to the actual turbine blades operational conditions. Thermomechanical fatigue crack
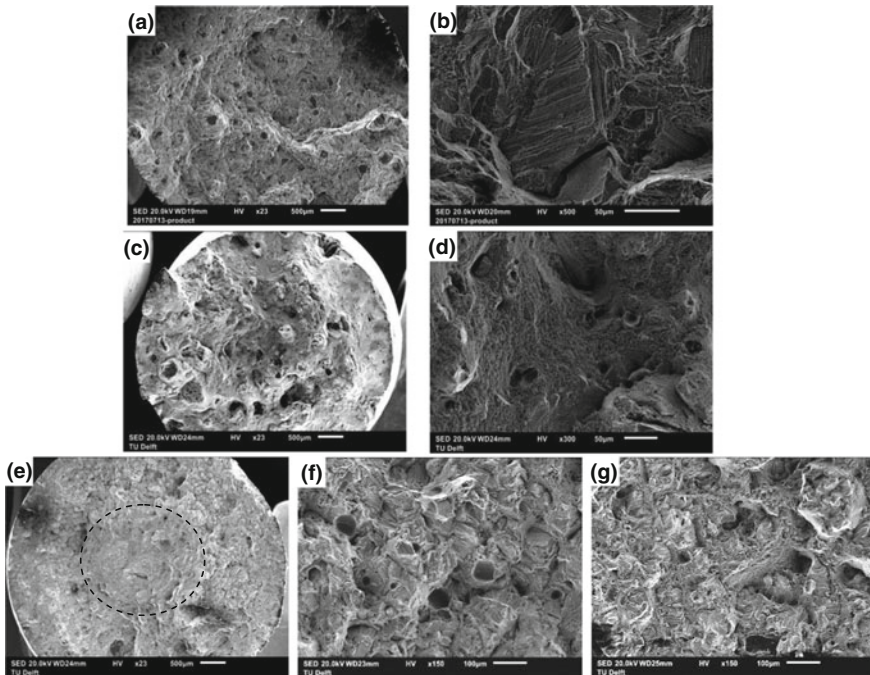

Fig. 6 Fracture surface of heat treated SLM produced Inconel 718 after creep testing at 650 °C and 690 MPa: **a** and **b** 250 W; **c** and **d** 950 W; **e** and **f** Functionally graded with core 950 W
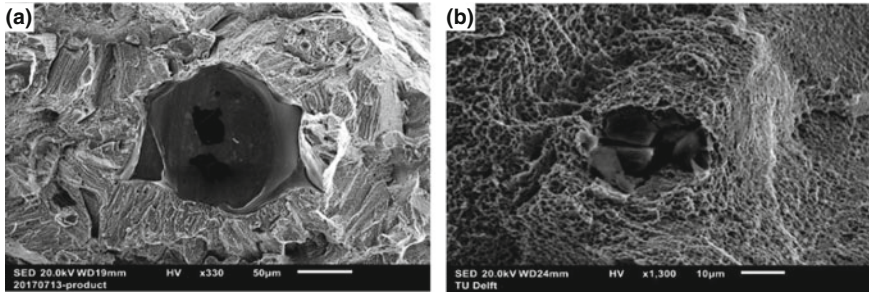
Fig. 7 Fracture surface of heat treated SLM produced Inconel 718, depicting **a** intergranular fracture around inclusion for 250 W and **b** ductile fracture around inclusion for 950 W

growth is more complicated than pure fatigue crack growth because it includes time dependent material behaviour characteristics such as creep and oxidation. Increasing temperature will activate specific mechanisms that can cause more damage than what would be expected by the individual contributions acting alone [15].

TMF results for fine and coarse grained SLM Inconel are shown in Table 4. As expected, samples produced with 950 W show short fatigue lifes as a result of large surface pores serving as crack initiation points. Cracks initiated at the surface pores result in a sudden force drop and final premature failure. On the other hand, samples produced with 250 W exhibit better TMF properties, which is explained by the small grain size and lower porosity. It should also be noted, that as heat-treated condition shows substantial increase in fatigue life. This lifetime increase can be explained by the dissolution of brittle Laves phase as well as the presence of the δ-phase at the grain boundaries, which provide restrictions to the grain boundary movement such as sliding [16]. Hence, grain boundary phases precipitated by heat treatment act as a barrier for dislocation motion, thus improving the high temperature properties of SLM built material.

An interesting observation was found for functionally graded material (FGM). As can be seen (Table 4), as-processed FGM samples show similar to pure matrix 250 W fatigue life properties, which indicates that outside shell (produced with fine grained 250 W) is the main microstructural zone controlling fatigue crack initiation

Table 4 In-phase thermomechanical fatigue (IP-TMF) data conducted between 350 and 650 °C

Specimen	Time until failure (h)	Cycles until failure	Porosity (%)
250 W–AP	103.3	621	1.1
250 W–HT	207.6	1246	1
950 W–AP	0.7	2	4.5
950 W–HT	45.7	275	4.1
FGM–AP	98.5	608	0.3
FGM–HT	407.2	2244	0.4

and growth and thus fatigue lifetime. A different fracture (crack growth) development has been observed for heat treated FGM sample, which shows superior to both 250 and 950 W lifetime properties. For this condition, during the initial 6 h under TMF loading, a pronounced decrease in developed tensile load levels has been observed, with a subsequent stabilisation. The load drop is indicating on specimen stiffness decrease due to the development of a TMF crack, whereas the load stabilization could be a result of possible crack arrest. Previous studies of nickel-based superalloys [17] showed that cracks which propagate along tortuous paths exhibit longer fatigue life than cracks with lesser deviation. Hence, obstructions such as grain boundaries, precipitates or graded interfaces may assist crack deflections into positions that cause crack arrest. This theory can explain behaviour of functionally graded material, where cracks that deviate into positions perpendicular to the loading direction (hence to core 950 W) no longer have a driving force to cause crack extension. Hence, instead of pure mode one loading of a crack growing perpendicular to the loading direction, small deviations create a mixed mode condition, decreasing the driving force, and slowing the crack growth rate. The proposed theory of crack arrest at graded interphase should be further investigated via fracture surface analysis and expended TMF testing. Furthermore, TMF testing of wrought Inconel should be performed in order to assess the possible benefits of AM functional grading.

Conclusions

A study of creep and thermomechanical fatigue of Inconel 718 produced by additive manufacturing has led to the following conclusions:

- *Post-processing heat treatment* in a form of solution treatment and double aging resulted in transformation of brittle Laves phase into a needle-like Ni_3Nb-δ precipitates.
- *Creep properties* of SLM produced Inconel do not show significant grain size effect, which might be attributed to high scatter in results caused by process induced pores observed in 950 W samples. Heat treatment, on the other hand, substantially improves creep properties, which is related to dissolution of Laves phase and precipitation hardening by plates of δ-phase, acting as a barrier for dislocation motion.
- There are two different *fracture mechanisms* observed in crept specimens: ductile fracture for 950 W and intergranular fracture for 250 W. It is suggested, that there is insufficient time for creep mechanisms initiation in 950 W samples exhibiting high density of process induced defects.
- *Thermomechanical fatigue* life of 950 W is lower than that of 250 W, which is due to larger grains and surface pores serving as crack initiation points. Heat treatment increases fatigue life by a factor of two.

- As-processed *functionally graded material* shows similar to pure matrix 250 W fatigue life, indicating that outside shell (produced with fine grained 250 W) is the main fatigue crack controlling zone.
- A substantial increase in *TMF lifetime* (by a factor of 4) is observed for *heat treated FGM condition*. A theory is proposed where functionally graded interface allows cracks to deviate into positions perpendicular to the loading direction (hence to core 950 W) thus reducing the driving force for further crack extension.

Further investigations of fracture surfaces as well as expended TMF testing will be performed in order to fully assess the possible benefits of AM functional grading.

References

1. Akca E, Gursel A (2015) A review on superalloys and IN718 nickel-based INCONEL superalloy. Periodicals Eng Nat Sci 3(1)
2. Azadian S, Wei LY, Warren R (2004) Delta phase precipitation in Inconel 718. Mater Charact 53(2004):7–16
3. Guedou J-Y et al (2008) Development of a new fatigue and creep resistant PM nickel-base superalloy for disk applications. In: Reed RC et al (eds) Superalloys 2008, TMS, Warrendale, PA, USA, pp 21–30
4. Murr LE, Gaytan SM et al (2012) Metal fabrication by additive manufacturing using laser and electron beam melting technologies. J Mater Sci Technol 28:1–14
5. Song B, Zhao X, Li Sh et al (2015) Differences in microstructure and properties between selective laser melting and traditional manufacturing for fabrication of metal parts: a review. Front. Mech. Eng. 10(2):111–125
6. Sames WJ, List FA, Pannala S, Dehoff RR, Babu SS (2016) The metallurgy and processing science of metal additive manufacturing. Int Mater Rev
7. Petch NJ (1953) J Iron Steel Inst 174:25
8. Moiz M (2013) The influence of grain size on the mechanical properties of Inconel 718. Linköping University, Sweden
9. Popovich VA, Borisov EV et al (2017) Functionally graded Inconel 718 processed by additive manufacturing: crystallographic texture, anisotropy of microstructure and mechanical properties. Mater Des 114:441–449
10. Popovich VA, Borisov EV et al (2017) Impact of heat treatment on mechanical behaviour of Inconel 718 processed with tailored microstructure by selective laser melting. Mater Des 131:12–22
11. AMS5664E Nickel Alloy, Corrosion and Heat Resistant, Bars, Forgings, and Rings 52.5Ni - 19Cr - 3.0Mo - 5.1Cb - 0.90Ti - 0.50Al - 18Fe Consumable Electrode or Vacuum Induction Melted 1950 °F (1066 °C) Solution Heat Treated, Precipitation Hardenable (2006)
12. E139 – 11, Standard Test Methods for Conducting Creep, Creep-Rupture, and Stress-Rupture Tests of Metallic Materials (2011)
13. Thébaud L et al (2015) Relationships between microstructural parameters and time-dependent mechanical properties of a new nickel based superalloy AD730™. In: Superalloys 2016, Wiley, pp 877–886
14. Reed RC (2006) The superalloys: fundamentals and applications. Cambridge University Press, Cambridge, UK

15. Zhang P, Zhu Q et al (2015) Review on thermo-mechanical fatigue behavior of nickel-base superalloys. Mater Trans 56(12):1930–1939
16. Baufeld B (2012) Mechanical properties of INCONEL 718 parts manufactured by shaped metal deposition (SMD). J Mater Eng Perform 21(7):1416–1421
17. Boyd-Lee AD (1999) Fatigue crack growth resistant microstructures in polycrystalline Ni-base superalloys for aeroengines. Int J Fatigue 21(4):393–405